INSIGHT INTO EFFECT OF MESO-SCALE VORTEX ON VERY-LARGE SCALE MOTION IN REAL NEUTRALLY STRATIFIED ATMOSPHERIC SURFACE LAYER WITH LES BY NUMERICAL WEATHER PREDICTION MODEL

Yasuo Hattori
Civil enginnering research laboratory
Central Research Institute of Electric Power Industry
1646 Abiko, Abiko-shi, Chiba-ken, 270-1194, Japan
yhattori@criepi.denken.or.jp

Keisuke Nakao
Civil enginnering research laboratory
Central Research Institute of Electric Power Industry
1646 Abiko, Abiko-shi, Chiba-ken, 270-1194, Japan
nakao@criepi.denken.or.jp

Hitoshi Suto
Civil enginnering research laboratory
Central Research Institute of Electric Power Industry
1646 Abiko, Abiko-shi, Chiba-ken, 270-1194, Japan
suto@criepi.denken.or.jp

Hiromaru Hirakuchi
Civil enginnering research laboratory
Central Research Institute of Electric Power Industry
1646 Abiko, Abiko-shi, Chiba-ken, 270-1194, Japan
hiromaru@criepi.denken.or.jp

ABSTRACT

The study of turbulence structures in the atmospheric surface layer (ASL) under near-neutral conditions have become active of late; the observation campaigns have revealed the existence of very-large-scale motions (VLMSs) in the wall turbulence under high Reynolds number conditions. However, the generation process of the VLMSs are not fully understood. Indeed, two conception models which differ in kind from each other are proposed in explanation for the origin, i.e., one is based on the top-down processes of the detached eddies with meso-scale vortices above the ASL and the other is based on the bottom up processed of attached eddies near the ground. The study here examine the impacts of meso-scale vortices above the ASL (logarithmic layer) to the VLSMs. We carried out a large-eddy simulation by using a numerical weather prediction model, WRF, for a real near-neutrally stratified ASL, and investigated the turbulence characteristics in the ASL, especially paying attention to the effects of impinging motion of detached eddies with meso-scale vortices above the ASL into the near-wall (ground) region. After confirming the basic characteristics of atmospheric turbulence in the ASL, which correspond to those generally observed in the ASL, and the height of the logarithmic layer (ASL) is about 10^2m, we discussed the temporal and spatial structures of fluctuating velocity fields through spectrum analysis, visualization of flow fields and conditional sampling procedures. The pre-multiplied energy spectrum of fluctuating streamwise velocity near the ground showed a characteristic length, which corresponds to VLSMs. The snapshots of instantaneous velocities present a streaky structures near the ground (in the ASL) and also the large-scale features above the ASL, which have a superimposed footprint in the small-scale structures near the ground. Two point correlations with time delay, $\Delta\tau$, between streamwise and vertical fluctuating velocities with the probing (reference) point fixed above the ASL, show the impact of impingements of detached eddies to the streamwise large-scale fluid motions of fluctuating velocities near the ground, e.g., the correlation of $R_{wu}(z, \Delta\tau)$ takes negative values in the ASL, the scale of which corresponds to that of VLSMs. These results give an evidence for the existence of interaction between impingement detached eddies with meso-scale vortices and the VLSMs in streamwise fluctuating velocities near-

wall (ground) region, and also imply the coexistence of conflicting two mechanism due to top-down and bottom up processes with the VLSMs in a real neutral ASL, which is consistent with the existing observations.

INTRODUCTION

The study of turbulence structures in the atmospheric surface layer (ASL) under near-neutral conditions, which is a lower part of the atmospheric boundary layer, has become active of late. The existing studies, mainly focusing on coherence structures of a wall turbulence under high Reynolds number conditions, have revealed the existence of very-large-scale motions (VLSMs) and their typical features, such as peaks occurring at low frequencies in the pre-multiplied energy spectra, through the observations (e.g. Hutchins and Marusic 2007, Wang and Zheng 2016).

Also, accurate descriptions for turbulence statistics of wind fields in the near-neutral ASL is critically required in view of the increasing and broadening use of numerical weather prediction models. The models need to estimate turbulence fluxes of momentum, heat and moisture in the ASL as boundary conditions. On the other hand, recent observations (Högström 1990, Högström et al. 2002, Drobinski et al. 2004, Drobinski et al. 2007) have indicated that the fluxes under near-neutral conditions are often inconsistent with Monin-Obukhof theory, which has been widely used in the models; the observations were conducted over flat surfaces with homogeneous roughness, and thus the violation from the theory might not be due to the underlying surface conditions.

Possible mechanisms for such deviations from Monin-Obukhof theory have been investigated with the help of rapid distortion theory and large eddy simulations (Högström et al. 2002, Carlotti and Drobinski 2004, Foster et al. 2006, Drobinski et al. 2007). These studies suggest that effects of detached eddies with “meso-scale vortices”, the characteristics length of which is much larger than those generated by the wind shear in the ASL, on the ASL are essential to the peculiar turbulence characteristics; detached eddies with “meso-scale vortices” might produce eddy impingements onto the ASL; as they descend into the ASL, they are strongly distorted by the local shear and impinge onto the ASL and change the vertical turbulence transport non-locally.

However, how detached eddies interact with turbulence structures in the ASL is not fully understood; indeed, there has been no clear evidence to show impinging eddy motions that might be key in the ASL and more work is eagerly awaited (Drobinski et al. 2007). In particular, the details of dynamic process, such as generation and disappearance of organized motions with the effects or detached eddies, has not been fully understood yet. This must be due to the lack of the information on spatial- and temporal-structures in the ASL with the observations, which is caused by the difficulty in measuring or including detached eddies in observations. Indeed, two conception models which differ in kind from each other are proposed in explanation for the origin of peaks in the pre-multiplied energy spectra (Högström et al. 2002, Hutchins and Marusic 2007), and also the possible mechanism for the generation of the VLSMs is still a matter of controversy (Hutchins et al. 2012, Fang and Porté-Agel 2015, Wang and Zheng 2016).

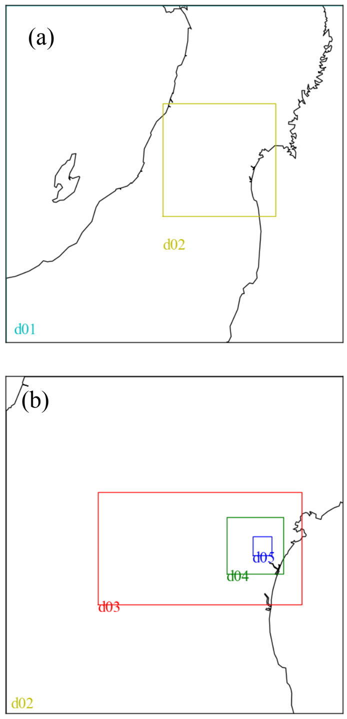

Figure 1. Computational domain for meso- (d01 and d02), (a) and micro-scale (d03 – d-5), (b) simulations.

Thus, aiming to investigate the effects of meso-scale vortices on the VLSMs in a real near-neutral atmospheric surface layer, we perform numerical simulations by using a mesoscale meteorological model, WRF, which has been widely used all over the world for numerical weather prediction, with LES mode (hereafter WRF-LES). We use a nesting technique, which represents the interaction between mesoscale vortices and turbulence eddies, such as setting for computational grids and domains and discuss turbulence structures in a real ASL under near neutral conditions.

EXPERIMENTAL SETUP

We consider a typical ASL turbulence under near-neutral conditions with a windstorm observed in Japan on April 3, 2012. The windstorm yielded strong wind fields with a constant wind direction over an area encompassing the Tohoku region during 6 hours, which must allow for the discussion on very large-scale coherence structures. The simulations are run for 6 hours with initialization at 1800 UTC, April 3, 2012, and the statistics are estimated with averaging over the last 20 min of the simulations.

We set-up the configurations in accordance with Talbot et al. (2012), which examined the performance of nested WRF-LES to explicitly simulate a spectrum of scales from large-scale mesoscale flow, down to fine scale turbulent eddies in the atmospheric boundary layer: the mesoscale simulation and the WRF-LES are run separately (mesoscale inputs are saved and later use to

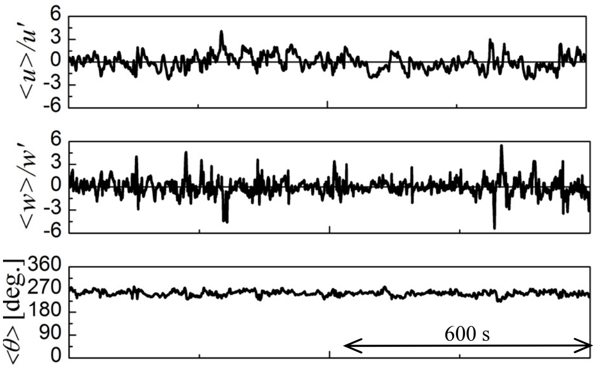

Figure 2. Time-series of fluctuating streamwise and vertical velocities normalized with r.m.s. values and wind direction at z = 10 m of the centre location in d05.

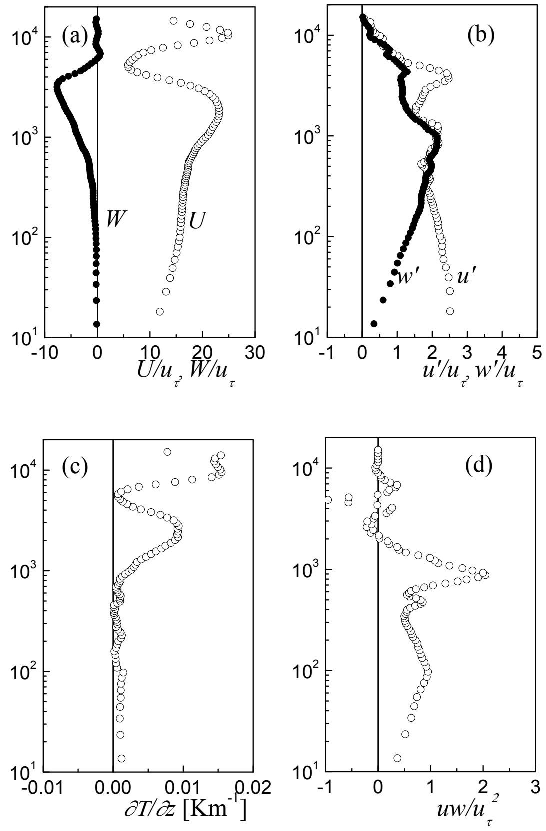

Figure 3. Vertical profiles of streamwise velocity for time averaged (a), and r.m.s. (b) values, time averaged potential temperature gradient and Reynolds shear stress at the centre location of d05.

force the WRF-LES), and thus, the one-way nesting is performed. The computational domains for the mesoscale simulation and WRF-LES are shown in Fig. 1. Five domains were nested for the simulation. The largest and coarsest two domains are set for the mesoscale simulation, while in the smallest and finest three with the nesting ratio of 1/3 the large-eddy simulation technique is used. The largest domain (d01) with a horizontal resolution of 1350 m extends over the entire Tohoku area in Japan so that the large-scale flow pattern can be realistically simulated. The innermost domain (d05), which has a horizontal resolution of 5.6 m, is covered by a flat terrain. All simulations have 96 vertical levels and the vertical stretching, and the first grid point is located approximately 6 m above the ground level on average, resulting in an innermost domain aspect ratio (horizontal grid size to vertical grid size) consistent with previous LES studies.

In the WRF-LES, we choose a fifth- and a third-order differencing schemes for the horizontal and vertical advection terms, respectively, while time integration is performed using a third-order Runge-Kutta scheme with small time steps. The 3-dimensional eddy viscosity predicted by the TKE equation for the 1.5 order turbulence closure is used to represent subgrid-scale diffusion and no PBL scheme is used. On the other hand, for the coarse domains (d01 and d02), the isotropic turbulence assumption is no longer valid, and thus, the YSU planetary boundary layer scheme was activated to account for the transport associated with the sub-grid mixing processes.

The evolution of parameters of relevance to the surface energy balance and surface water balance such as soil moisture, surface skin temperature, and heat fluxes are computed during the simulation by the unified Noah land-surface model. The chosen longwave and shortwave radiation schemes are the Rapid Radiative Transfer Model (RRTM) and Dudhia scheme, respectively. Cloud microphysics is parameterized using the WSM 6-class graupel scheme; essentially, the microphysical scheme does not affect the results on the turbulence structures, because the event did not accompany with precipitation.

The input data is prepared using a modified pre-processor based on the WRF Pre-processing System (WPS) to handle Japanese GPV and geographical datasets in our numerical weather forecasting and analysis system (Hashimoto and Hirakuchi 2010). Meteorological initial and boundary conditions are set to the coarsest domain using a mesoscale reanalysis product provided by Japan Meteorological Agency. The geographical data for the land use and topography are obtained from the Geospatial Information Authority of Japan dataset and have resolutions of 100 m for the land use and 50 m for topography.

RESULTS

Figure 2 shows the time-series of fluctuating streamwise and vertical velocities normalized with r.m.s values and wind direction in the ASL (at $z \cong 10$ m of the centre location in d05). Here, we should stress that the sub-grid scale components are firstly set to zero in nesting procedures, while grid scale components are interpolated in time and space in the simulations. This requires the sufficient spin-up time to obtain the steady states. These time-series do not show the tendency to increase or decrease against time, implying a quasi-steady PBL, and also satisfy the criteria for data selection to discuss the

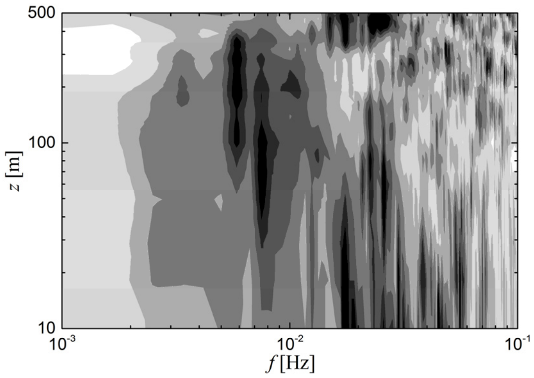

Figure 4. Pre-multiplied energy spectrum of fluctuating streamwise velocity at the centre location of d05.

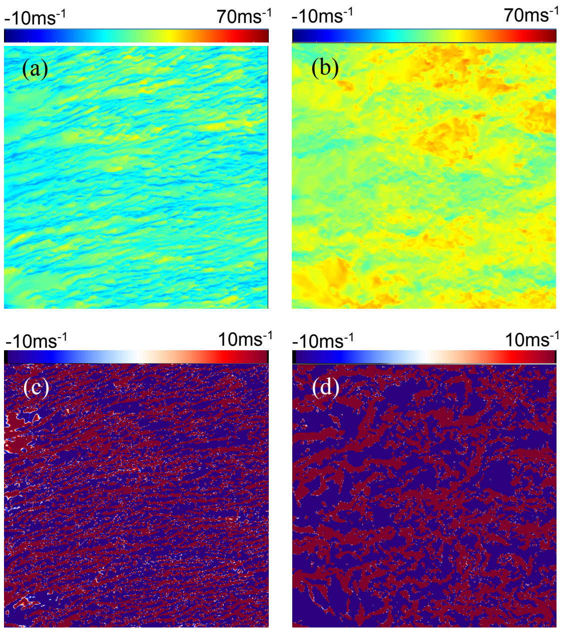

Figure 5. Instantaneous streamwise and vertical velocities, u and w, in the horizontal plate of d05 (7.5 km × 7.5 km) at two different height: (a) and (b) are for u at $z \cong 10$ m and $z \cong 150$ m (above the ASL); (c) and (d) are for w at $z \cong 10$ m and $z \cong 150$ m (above the ASL).

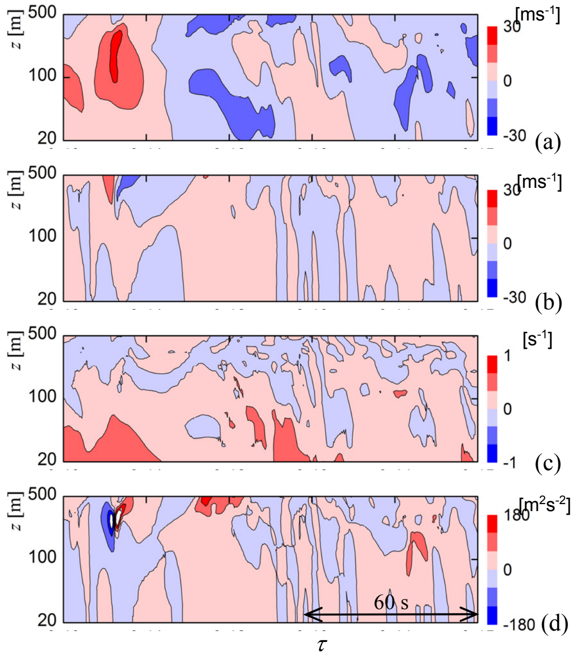

Figure 6. Example of time-height contours of streamwise (a) and vertical (b) fluctuating velocities, wind shear, (c) and Reynolds shear stress, (d) at the centre location of d05.

turbulence structures with the real-site observations proposed by Hutchins et al. (2012).

Figure 3 shows the vertical profiles of streamwise velocity for time averaged and r.m.s. values at the centre location of d05. The profiles of potential temperature gradient and the Reynolds shear stress are also shown in the figure. The statistics of velocities are normalized with friction velocity, u_τ. The streamwise velocity shows the logarithmic profile for the boundary layer beneath $z \cong 100$ m, where the vertical velocity and potential temperature gradient become almost zero. These profiles indicate that the ASL of present simulations has a typical turbulence characteristics under near-neutral conditions with the layer thickness of 10^2 m, which yield negligibly small buoyant effects. Also, the maximum r.m.s. values qualitatively agree with observations (Hattori et al. 2010) which give the values of 2 – 3 for streamwise component and 1 – 2 for vertical component. This implies that the grid resolutions used in the present study is much fine to represent turbulence statistics near the ground. Indeed, the values of TKE near the ground normalized with the friction velocity were about 30% of the values of grid scale components. Note that, detailed study of subgrid-scale modelling and its effects on predicted turbulence structures is beyond the scope of this paper.

Figure 4 depicts pre-multiplied energy spectrum of fluctuating streamwise velocity at the centre location of d05 with inner flow scaling against the frequency. The energy containing range is fully resolved as well as a small portion of spectra with -2/3 slope (compensated spectrum), corresponding to the discussion on predicted turbulence intensities in Fig. 3. The lowest frequency for -2/3 slope, which agrees well with observations (Drobinski et al. 2007) with a plateau in the middle frequency range. Also, the spatial scale estimated with frequencies for the plateau, corresponds to the very large-scale coherent structures, the scale of which is 10^2 m – 10^3m, reported with observations (Hutchins and Marusic 2007). Thus, the spectrum in the middle frequency ranges must be related to the VLSMs (Hutchins and Marusic 2007) and also the impingement of meso-scale vortices on the ASL.

Figure 5 depicts contour of instantaneous values of streamwise and vertical velocities in the horizontal plane of d05 (7.5km × 7.5km in area) at $z \cong 10$ m (near the ground) and $z \cong 150$ m (above the logarithmic layer, ASL).

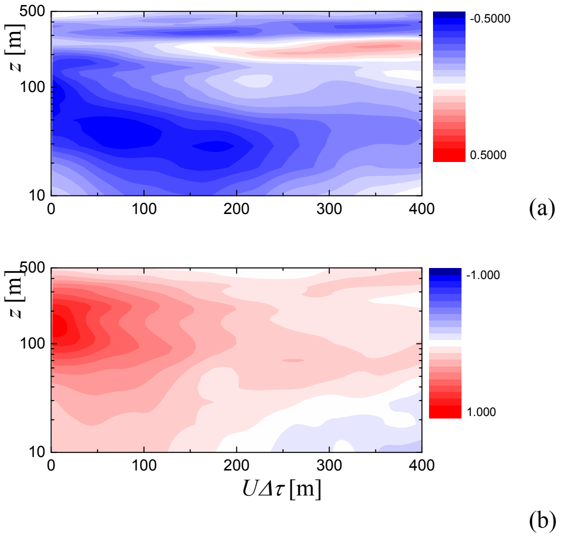

Figure 7. Two point correlations with time delay $\Delta\tau$ between streamwise and vertical fluctuating velocities, R$wu(z, \Delta\tau)$, (a), and R$ww(z, \Delta\tau)$, (b), at the centre location of d05; the probing point for vertical fluctuating velocities is fixed at $z \cong 150$ m (above the ASL) and the correlations are calculated for $w < -w'$ at probing point; the correlations are shown in the relationship between z and $U\Delta\tau$.

The snapshots at $z \cong 10$ m present the streaky structures with highly elongated regions of uniform streamwise momentum. The large-scale features at $z \cong 150$ m have a superimposed footprint in the small-scale structures at $z \cong 10$ m, implying the interaction of coherence structures in and above the ASL.

Figure 6 shows the typical example of time evolution of vertical profiles of streamwise and vertical fluctuating velocities, wind shear and Reynolds shear stress at the centre location of d05 for 2 min., which corresponds to 3 – 10 km in length scale with Taylor hypothesis of frozen turbulence, which must be applicable for capturing VLSMs (Dennis and Nickels 2008). The time evolution gives the transition process in the ASL from the impingement of high momentum fluids to bursting of low momentum fluids. The former motions strengthen the wind shear near the ground, whereas the latter motions have little dramatic impacts on the shear. Nevertheless, the Reynolds shear stress is mainly generated with the latter motions.

Figure 7 shows two point correlations with time delay $\Delta\tau$ between streamwise and vertical fluctuating velocities, R$wu(z, \Delta\tau)$ and R$ww(z, \Delta\tau)$ at the centre location of d05. To discuss the effects of detached eddies with meso-scale vortices, the probing (reference) point for vertical fluctuating velocities to calculate the correlation coefficients is fixed to $z \cong 150$ m, which is located above the logarithmic layer (ASL). Also the correlations are calculated with conditional sampling procedure, i.e., the correlation coefficients are calculated for the fluctuating velocities under $w < -w'$ at probing point. The correlations are shown in the relationship between z and $U\Delta\tau$, corresponding to the vertical- and streamwise-directions with Taylor hypothesis of frozen turbulence (Dennis and Nickels 2008). The distribution of R$wu(z, \Delta\tau)$ clearly shows the impacts of sweep-like motions to the streamwise velocity fluctuation near the ground (wall): the R$wu(z, \Delta\tau)$ takes negative values in the logarithmic layer. The negative value region has the length of 10^2 m in the streamwise direction, which agree well with the characteristics length of VLSMs (Hutchins and Marusic 2007, Huthincs et al. 2012). On the other hand, the R$ww(z, \Delta\tau)$ near the ground takes small values (about zero), indicating that such sweep events do not essentially generate the Reynolds shear stress.

DISCUSSION AND CONCLUSIONS

The study here examine the impacts of meso-scale vortices above the ASL (logarithmic layer) to a coherence structure near the ground under high Re number conditions, “very large scale motions” (VLSMs). We carried out a large-eddy simulation by using a numerical weather prediction model, WRF, for a real near-neutrally stratified ASL, and investigated the turbulence characteristics in the ASL, especially paying attention to the effects of impinging motion of detached eddies with meso-scale vortices above the ASL into the near-wall (ground) region.

Firstly, we confirmed the basic characteristics of atmospheric turbulence in the ASL, such as time-series of fluctuating velocities and vertical profiles of turbulence statistics, which correspond to those generally observed in the ASL, and the height of the logarithmic layer (ASL) is about 10^2m. Then, we discussed the temporal and spatial structures of fluctuating velocity fields through spectrum analysis, visualization of flow fields and conditional sampling procedures. The pre-multiplied energy spectrum of fluctuating streamwise velocity near the ground showed a plateau in the middle frequency range with the spatial scale of 10^2m – 10^3 m, which corresponds to VLSMs (Hutchins and Marusic 2007). The snapshots of instantaneous velocities present a streaky structures with highly elongated regions of uniform streamwise momentum near the ground (in the ASL) and the large-scale features above the ASL, which have a superimposed footprint in the small-scale structures near the ground. The time evolution of vertical profiles of streamwise and vertical fluctuating velocities, wind shear and Reynolds shear stress and the two point correlations with time delay between streamwise and vertical fluctuating velocities with the probing (reference) point fixed above the ASL, show the impact of impingements of detached eddies to the streamwise large-scale fluid motions of fluctuating velocities near the ground, e.g., the correlation of R$wu(z, \Delta\tau)$ takes negative values in the ASL, the scale of which corresponds to that of VLSMs.

From these results, we found the effects of impingement detached eddies with meso-scale vortices on the VLSMs in streamwise fluctuating velocities near-wall (ground) region, which has a characteristic length of 10^2 m – 10^3 m. Also, we implied the coexistence of conflicting two mechanism due to top-down and bottom up processes with the VLSMs in a real neutral ASL, which is consistent with the existing observations (Hutchins et al. 2012, Wang and Zheng 2016). The energy spectrum and snapshots of streamwise velocity at different heights, including the locations above the ASL suggest the impacts of the meso-scale vortices on the VLSMs in the ASL.

The authors are deeply indebted to the anonymous reviews for useful comments on the extended abstract. The authors also thank Mr. Shuji Ishihara of DCC, Dr. Atsushi Hashimoto and Dr. Mitsuharu Nomura for his careful assistance in numerical simulations. This work was performed under the support of collaboration between NCAR and CRIEPI; the authors acknowledge Dr. Chin-Hoh Moeng of NCAR for valuable discussion and wish to express our gratitude to Dr. Sun, Juan Zhen and Dr. Soichiro Sugimoto for helps of the collaboration between NCAR.

REFERENCES

Carlotti, P., and Drobinski, P., 2004, "Length scales in wall- bounded high-Reynolds-number turbulence", *J Fluid Mech*, Vol. 516, pp.239-264.

Dennis, D.J.C., and Nickels, T.B., 2008, "On the limitations of Taylor's hypothesis in constructing long structures in a turbulent boundary layer", *J Fluid Mech*, Vol.614, pp.197-206.

Drobinski, P., Carlotti, P. Newsom, R.K., Banta, R.M., Foster, R.C., and Redelsperger, J-L., 2004, "The structure of the near-neutral atmospheric surface layer", *J Atmos Sci*, Vol. 61, pp.699-714.

Drobinski, P., Carlotti, P., Redelsperger, J-L., Banta, R.M., Masson, V., and Newsom, R., 2007 "Numerical and experimental investigation of the neutral atmospheric surface layer", *J Atmos Sci*, Vol. 64, pp.137-156.

Fang, J., and Porte-Agel, F., 2015, "Large-eddy simulation of very-large scale motions in the neutrally stratified atmospheric boundary layer", *Boundary-Layer Meteorol*, Vol. 155, pp. 397-416.

Foster, R.C., Vianey, F., Drobinski, P., and Carlotti, P., 2006, "Near-surface coherent structures and the vertical momentum flux in a large-eddy simulation of the neutrally-stratified boundary layer", *Boundary-Layer Meteorol*, Vol. 120, pp.229-255.

Hashimoto, A., and Hirakuchi, H., 2010, "Enhancement and accuracy evaluation of Numerical Weather Forecasting and Analysis System (NuWFAS) for the Hokkaido Island", CRIEPI report N09024. (*in Japanese*)

Hattori, Y., Moeng, C-H. Suto, H., Tanaka, N., and Hirakuchi, H., 2010, "Wind-tunnel experiment on logarithmic-layer turbulence under the influence of overlying detached eddies", *Boundary-Layer Meteorol*, Vol. 134, pp.269-283.

Högström, U., 1990, "Analysis of turbulence structure in the surface layer with a modified similarity formulation for near neutral conditions", *J Atmos Sci*, Vol. 47, pp. 1949-1972.

Högström, U., Hunt. J.C.R., and Smedman, A-S., 2002, "Theory and measurements for turbulence spectra and variances in the atmospheric neutral surface layer", *Boundary-Layer Meteorol*, Vol. 103, pp.101-124.

Hutchins, N., and Marusic, I., 2007, "Evidence of very long meandering features in the logarithmic region of turbulent boundary layers", *J Fluid Mech*, Vol. 579, pp. 1-28.

Hutchins, N., Chauhan, K., Marusic, I., Monty, J., and Klewicki, J., 2012, "Towards reconciling the large-scale structure of turbulent boundary layers in the atmosphere and laboratory", *Boundary-Layer Meteorol*, Vol. 145, pp. 273-306.

Talbot, C., Bou-Zeid, and E., Smith, J. 2012, "Nested mesoscale large-eddy simulations with WRF: Performance in real test cases", *J Hydrometeorol*, Vol. 13, pp. 1421-1441.

Wang, G., and Zheng, X., 2016, "Very large scale motions in the atmospheric surface layer: a field investigation", *J Fluid Mech*, Vol. 802, pp. 464-489.